Relevance of Electrokinetic Theory for "Soft" Particles to Bacterial Cells: Implications for Bacterial Adhesion

Alexis J. de Kerchove and Menachem Elimelech*

Department of Chemical Engineering, Environmental Engineering Program, Yale University, P.O. Box 208286, New Haven, Connecticut 06520-8286

Received December 1, 2004. In Final Form: April 18, 2005

Bacterial cells and other biological particles carry charged macromolecules on their surface that form a "soft" ion-permeable layer. In this paper, we test the applicability of an electrokinetic theory for soft particles to characterize the electrophoretic mobility (EPM) and adhesion kinetics of bacterial cells. The theory allows the calculation of two parameters—the electrophoretic softness and the fixed charged density—that define the characteristics of the polyelectrolyte layer at the soft particle surface. The theory also allows the calculation of an outer-surface potential that may better predict the electrostatic interaction of soft particles with solid surfaces. To verify its relevance for bacterial cells, the theory was applied to EPM measurements of two well-characterized *Escherichia coli* K12 mutants having lipopolysaccharide (LPS) layers of different lengths and molecular compositions. Results showed that the obtained softness and fixed charge density were not directly related to the known characteristics of the LPS of the selected strains. Interaction energy profiles calculated from Derjaguin−Landau−Verwey−Overbeek (DLVO) theory were used to interpret bacterial deposition (adhesion) rates on a pure quartz surface. The outer surface potential failed to predict the low attachment efficiencies of the two bacterial strains. The lack of success in the application of the theory for soft particles to bacterial cells is attributed to chemical and physical heterogeneities of the polyelectrolyte layer at the cell surface.

1. Introduction

A fundamental understanding of the interactions between bacterial cells and solid interfaces is of paramount importance in many fields of science and engineering.[1−4] In a liquid environment rich in nutrients—such as, tears, saliva, human serum, lymph, or wastewater—bacterial adhesion results in the development of a biofilm by the rapid growth of the bacterial population.[5] The formation of biofilms on surfaces, a process referred to as biofouling, is a major problem causing the direct dysfunction of the fouled devices.[1,6]

In several biomedical applications, surfaces are developed to be accepted by the human body in such way that human cells can colonize the device surface faster than exogenous bacteria species.[1] Examples of such surfaces include dental implants,[7] contact lenses,[8] prostheses,[9] ureteral stents,[10] and catheter.[11] Biofouling is also a major problem in engineered systems, including membranes in water and wastewater treatment units,[12,13] ship hulls,[14] and heat exchangers.[15] Bifouling remains a major challenge because of the intricate processes and mechanisms involved in bacterial deposition, growth, and community development. Due to the complexity and persistence of biofilms, prevention strategies focus mainly on the control of bacterial adhesion.[16] Hence, a better understanding of the bacterial cell surface characteristics is needed to predict and control bacterial adhesion.

Under controlled laboratory conditions, the initial adhesion (deposition) kinetics of model colloidal particles have often been explained by the classic Derjaguin−Landau−Verwey−Overbeek (DLVO) theory.[17−21] This theory predicts the total interaction energy between the particle and a collector surface as the sum of van der Waals and electrostatic double layer interactions. Accurate determination of the electrostatic double layer interaction between the particle and collector surface plays a crucial role in prediction of particle deposition kinetics. An important parameter for the calculation of the electrostatic double layer interaction is the electrical surface potential of the particles. For hard spherical particles, the surface potential is often approximated by the zeta potential, the potential located at the electrokinetic plane of shear. The latter can be readily determined for hard particles from electrophoretic mobility (EPM) measurements.[22−26]

* Corresponding author. Phone: (203)432-2789. Fax: (203)432-2881. E-mail: menachem.elimelech@yale.edu.

(1) Gottenbos, B.; Busscher, H. J.; van der Mei, H. C. *J. Mater. Sci.: Mater. Med.* **2002**, *13*, 717−722.
(2) Gristina, A. G. *Science* **1987**, *237*, 1588−1595.
(3) Melo, L. F.; Bott, T. R. *Exp. Therm. Fluid Sci.* **1997**, *14*, 375−381.
(4) Tufenkji, N.; Ryan, J. N.; Elimelech, M. *Environ. Sci. Technol.* **2002**, *36*, 422A-428A.
(5) Costerton, J. W.; Lewandowski, Z.; Caldwell, D. E.; Korber, D. R.; Lappinscott, H. M. *Annu. Rev. Microbiol.* **1995**, *49*, 711−745.
(6) Flemming, H. C.; Schaule, G.; Griebe, T.; Schmitt, J.; Tamachkiarowa, A. *Desalination* **1997**, *113*, 215−225.
(7) Yang, J. L.; Bos, R.; Belder, G. F.; Engel, J.; Busscher, H. J. *J. Colloid Interface Sci.* **1999**, *220*, 410−418.
(8) Bruinsma, G. M.; van der Mei, H. C.; Busscher, H. J. *Biomaterials* **2001**, *22*, 3217−3224.
(9) Jones, D. S.; McGovern, J. G.; Adair, C. G.; Woolfson, A. D.; Gorman, S. P. *J. Mater. Sci.: Mater. Med.* **2001**, *12*, 399−405.
(10) Denstedt, J. D.; Reid, G.; Sofer, M. *World J. Urol.* **2000**, *18*, 237−242.
(11) Gorman, S. P.; Jones, D. S.; Mawhinney, W. M.; McGovern, J. G.; Adair, C. G. *J. Mater. Sci.: Mater. Med.* **1997**, *8*, 631−635.
(12) Flemming, H. C.; Schaule, G. *Desalination* **1988**, *70*, 95−119.
(13) Ridgway, H. F.; Flemming, H. C. In *Water treatment Membrane Processes*; Mallevialle, J., Odendaal, P. E., Wiesner, M. R., Eds.; McGraw-Hill: New York, 1996; pp 6.1−6.62.
(14) Murugan, A.; Ramasamy, M. S. *Indian J. Mar. Sci.* **2003**, *32*, 162−164.
(15) Melo, L. F.; Vieira, M. J. *Bioprocess Eng.* **1999**, *20*, 363−368.
(16) Meyer, B. *Int. Biodeterior. Biodegrad.* **2003**, *51*, 249−253.
(17) Hunter, R. J. *Foundation of Colloid Science*; Oxford University Press: Oxford, 2001; Vol. 2.
(18) Bellmann, C. *Chem. Ing. Technol.* **2003**, *75*, 662−668.
(19) Adamczyk, Z. *Adv. Colloid Interface Sci.* **2003**, *100*, 267−347.
(20) Overbeek, T. *Adv. Colloid Interface Sci.* **1999**, *83*, IX−XI.
(21) Hermansson, M. *Colloids Surf., B* **1999**, *14*, 105−119.
(22) von Smoluchowski, M. *Phys. Chem. (Muenchen, Ger.)* **1918**, *92*, 129.

10.1021/la047049t CCC: $30.25
Published on Web 06/02/2005

Bacteria as well as other types of biological cells carry on their surface charged polymers that form a "soft" ion-permeable layer around the cell.[27] For bacterial cells, these polymers mainly comprise lipopolysaccharides, proteins, and pili or fimbriae.[28] The presence of a polyelectrolyte layer on the cell controls the spatial distribution of the electric surface potential and the resulting interaction forces between a bacterial cell and solid surfaces. Most electrokinetic theories, being developed for ion-impermeable solid particles, are not suitable for such soft particles. Complex soft particles, like bacterial cells, call for new electrokinetic theories that take into account the presence of the ion-permeable polyelectrolyte layer.[29]

The most accepted electrokinetic theory for "soft" particles was developed by Ohshima.[30,31] Reasonable results were obtained when the theory was applied to latex particles covered with well-defined temperature-sensitive hydrogel layer.[32,33] The derived analytical solution approximates the potentials associated with the ion-permeable layer of the soft particle—the outer surface potential and the Donnan potential—from EPM measurements. The analytical expression derived by Ohshima consists of two terms. The first term is a weighted average of the outer surface potential and the Donnan potential, whereas the second term is directly related to the soft layer fixed charge and is independent of the shielding effect of the electrolyte. Based on the assumptions that the polyelectrolyte layer carries a uniform distribution of fixed charges and that it is uniformly permeable to the electrolyte solution, the theory defines two specific parameters: the *fixed charge density* and the *electrophoretic softness*. These parameters quantify the volumetric charge and the electrolyte permeability in the soft layer, respectively.

Ohshima's theory has been used to describe bacterial cell electrophoretic characteristics under specific environmental conditions or growth phase,[34−37] to depict the influence of surface features, such as lipopolysaccharides[38] and fimbriae,[39,40] on the obtained parameters of fixed charge and electrophoretic softness, and to predict interactions between bacterial cells and substrates, such as glass or biological interfaces.[41−43] However, despite the extensive use of Ohshima's electrophoretic theory for soft particles, the applicability of the theory to biological cells and the relevance of the calculated parameters to describe cell surface features have never been verified. In fact, recent studies involving bacterial strains with different surface features strongly suggest that "softness" parameters derived from the theory do not reflect the actual cell surface structure/morphology.[40] Hence, more systematic experimental studies are needed to investigate whether Ohshima's theory is applicable to characterize the softness of biological cells and to pinpoint the major shortcomings of the theory when applied to bacterial cells.

In this study, the electrophoretic mobilities of two well-characterized *Escherichia coli* strains having well-defined lipopolysaccharide molecules of different length and chemical composition were systematically investigated. EPM versus ionic strength data were used with Ohshima's theory to determine the electrophoretic softness and fixed charge density of the model bacterial strains. These parameters were related to the known features of the bacterial lipopolysaccharides to examine the relevance of Ohshima's theory to characterize bacterial cell surfaces. Furthermore, the outer surface potential of the bacterial strains at the investigated ionic strengths was calculated from the obtained fixed charged density. The outer surface potentials were used to determine the DLVO interaction energy between the bacterial cells and a quartz surface to evaluate whether the outer surface potentials can be used to predict bacterial attachment efficiencies.

2. Materials and Methods

2.1. Selection and Preparation of Model Bacterial Cells. Two well-characterized strains of *Escherichia coli* (*E. coli*) were selected as model bacterial cells for this electrokinetic study. The "rough" and "deep-rough" mutants of the *E. coli* K12 strain,[44] D21 and D21f2, were obtained from the *E. coli* Genetic Stock Center at Yale University. To allow cell detection under fluorescent microscopy, bacterial strains were tagged with a plasmid coding for green fluorescent protein.[45] The transformed GFP-expressing cell lines are referred to as D21g and D21f2g.

The two strains mainly differ in the length and composition of their LPS molecules.[46] The parent strain D21g produces LPS molecules having the lipid A, two 2-keto-3-deoxy-D-manno-octonic acid (KDO) molecules, and core polysaccharide, while D21f2g is an isogenic mutant of D21g with a truncated LPS molecule comprising lipid A and the two KDO molecules.[47] These genetically related mutants differ in their LPS length and charge density and thus represent ideal model strains to study the applicability of the electrophoretic theory for "soft" particles to bacterial cells. The equivalent diameters of D21g and D21f2g are 1.84 and 1.77 μm, respectively.[45] In addition to the bacterial cells, silica particles (Bangs Laboratory, Inc., Fishers, IN) with an average diameter of 1.59 μm were utilized as model hard, rigid spheres.

Cells were grown in Luria-Bertani broth (LB broth, Fisher, Fair Lawn, NJ) at 37 °C in the presence of 0.03 mg/L gentamicin (Sigma, St. Louis, MO) until reaching mid-exponential phase (3 h), at which time they were harvested for use. The cells were pelleted by centrifugation (Sorvall RC26 Plus Centrifuge) for 15 min at 3823*g* in a SS34 rotor (Kendro Laboratory Products, Newtown, CT). The growth medium was decanted, and the pellet was resuspended in a 10 mM KCl solution. This procedure of

(23) O'Brien, R. W.; White, L. R. *J. Chem. Soc., Faraday Trans.* **1978**, *74*, 1607−1626.
(24) Ohshima, H. *J. Colloid Interface Sci.* **1996**, *179*, 431−438.
(25) Ohshima, H. *J. Colloid Interface Sci.* **2001**, *239*, 587−590.
(26) Semenikhin, N. M.; Dukhin, S. S. *Colloid J. USSR*+ **1975**, *37*, 1017−1022.
(27) Ohshima, H.; Kondo, T. *Biophys. Chem.* **1991**, *39*, 191−198.
(28) Madigan, M. T.; Martinko, J. M.; Parker, J. *Brock biology of microorganisms*, 10th ed.; Prentice Hall, Pearson Education, Inc.: Upper Saddle River, NJ, 2003.
(29) vanderWal, A.; Minor, M.; Norde, W.; Zehnder, A. J. B.; Lyklema, J. *Langmuir* **1997**, *13*, 165−171.
(30) Ohshima, H.; Kondo, T. *J. Colloid Interface Sci.* **1989**, *130*, 281−282.
(31) Ohshima, H. *J. Colloid Interface Sci.* **1994**, *163*, 474−483.
(32) Ohshima, H.; Makino, K.; Kato, T.; Fujimoto, K.; Kondo, T.; Kawaguchi, H. *J. Colloid Interface Sci.* **1993**, *159*, 512−514.
(33) Makino, K.; Yamamoto, S.; Fujimoto, K.; Kawaguchi, H.; Ohshima, H. *J. Colloid Interface Sci.* **1994**, *166*, 251−258.
(34) Hayashi, H.; Seiki, H.; Tsuneda, S.; Hirata, A.; Sasaki, H. *J. Colloid Interface Sci.* **2003**, *264*, 565−568.
(35) Bos, R.; van der Mei, H. C.; Busscher, H. J. *Biophys. Chem.* **1998**, *74*, 251−255.
(36) Sonohara, R.; Muramatsu, N.; Ohshima, H.; Kondo, T. *Biophys. Chem.* **1995**, *55*, 273−277.
(37) Kiers, P. J. M.; Bos, R.; van der Mei, H. C.; Busscher, H. J. *Microbiology (Reading, U. K.)* **2001**, *147*, 757−762.
(38) Abu-Lail, N. I.; Camesano, T. A. *Environ. Sci. Technol.* **2003**, *37*, 2173−2183.
(39) Takashima, S.; Morisaki, H. *Colloids Surf., B* **1997**, *9*, 205−212.
(40) Rodriguez, V. V.; Busscher, H. J.; Norde, W.; van der Mei, H. C. *Electrophoresis* **2002**, *23*, 2007−2011.
(41) Poortinga, A. T.; Bos, R.; Busscher, H. J. *Colloids Surf., B* **2001**, *20*, 105−117.
(42) Morisaki, H.; Nagai, S.; Ohshima, H.; Ikemoto, E.; Kogure, K. *Microbiology (Reading, U. K.)* **1999**, *145*, 2797−2802.
(43) Tsuneda, S.; Jung, J.; Hayashi, H.; Aikawa, H.; Hirata, A.; Sasaki, H. *Colloids Surf., B* **2003**, *29*, 181−188.
(44) Snyder, S.; Kim, D.; McIntosh, T. J. *Biochemistry* **1999**, *38*, 10758−10767.
(45) Walker, S. L.; Redman, J. A.; Elimelech, M. *Langmuir* **2004**, *20*, 7736−7746.
(46) Berlyn, M. B.; Letovsky, S. *Nucleic Acids Res.* **1992**, *20*, 6143−6151.
(47) Boman, H. G.; Monner, D. A. *J. Bacteriol.* **1975**, *121*, 455−464.

pelleting and rinsing was repeated two additional times to remove traces of the growth medium. The electrolyte solutions were prepared with deionized water (Barnstead Thermolyne Corporation, Dubuque, IA) and reagent-grade KCl (Fisher) with no pH adjustment (pH 5.5−5.7).

2.2. Electrokinetic Characterization. The EPM of the bacterial cells was measured as a function of ionic strength by microelectrophoresis (ZetaPALS, Brookhaven Instruments Corp, Holtsville, NY) and processed by the provided software (ver. 3.13). EPM measurements were conducted over a broad range of ionic strengths, from 1 to 300 mM KCl, at ambient pH (5.5−5.7) and room temperature (22 °C).

2.2.1. Electrophoretic Mobility Measurement at High Ionic Strength. Settings (frequency, voltage, and relative residual) of the ZetaPALS analyzer were tested and verified at high ionic strengths using human erythrocytes as standard particles. It has been reported that human erythrocytes have a constant EPM of $-1.32\ \mu m\ s^{-1}\ V^{-1}\ cm$ (or $-1.32 \times 10^{-8}\ m^2\ V^{-1}\ s^{-1}$) in a 1/15 M PBS (75.6 mM ionic strength) at pH 7.4.[48] A human blood sample was collected prior to each EPM measurement and diluted in the buffer solution to reach a final concentration of 10^4-10^5 cells/mL. Five replicates or more were studied for each of the setting trials. The ZetaPALS analyzer showed the most accurate and reproducible EPM readings, with an EPM of $-1.32 \pm 0.03 \times 10^{-8}\ m^2\ V^{-1}\ s^{-1}$, at a frequency of 2.0 Hz, a voltage of 2.5 V, and relative residual from 0.01 to 0.02. The optimal frequency and voltage are identical to the frequency and voltage suggested in the automatic settings. It was further observed that EPM values were dependent on the conductance reading of the sample by the ZetaPALS instrument. The correct EPM for human erythrocytes is obtained when the successive conductance readings of the same sample give identical values, approaching the real conductance of the solution (measured independently by a separate conductance probe). Prior to each fresh sample, two to three conductance readings of the buffer solution were required to allow the polarization of the electrodes at the studied ionic strength and to obtain stable conductance readings. Measurements of bacterial EPM over the examined ionic strength range were thus obtained by first polarizing the electrodes, and by varying the relative residual as the ionic strength increases. Results were shown to be optimal when the relative residual had a value between 0.025 and 0.030 for low ionic strength (less than 30 mM), between 0.015 and 0.020 for intermediate ionic strength (between 30 and 90 mM), and between 0.005 and 0.010 for high ionic strength (greater than 90 mM).

2.2.2. Protocol for Bacterial Electrophoretic Mobility Measurement. Following the last rinse, the bacterial cell pellet was resuspended in 10 mM KCl solution to obtain a final concentration of 10^9 cells/mL and stored on ice. Cells were diluted 1000 times in a 5 mL solution of the desired ionic strength, with samples freshly prepared before each EPM measurement. For each sample, the measured EPM represents the average of 10 successive EPM readings of the ZetaPALS at the settings described in the previous subsection. The final bacterial EPM at each ionic strength is the weighted average of EPM measurements of 12 samples made out of 4 different cell cultures. Between EPM measurements, the electrode set was thoroughly rinsed, first with 75% ethanol followed by deionized water. EPM measurements of the silica particles were carried out in a similar way.

2.3. Ohshima's Electrokinetic Theory for "Soft" Particles. Although there were several efforts regarding electrokinetic theory for soft surfaces,[49,50] all have a common main feature—they are developed on the basis of Smoluchowski theory for hard surfaces. Smoluchowski theory is based on the Poisson−Boltzmann (PB) equation, which describes the diffuse portion of the double layer (DL), and the Stokes hydrodynamic equation. The latter includes an additional term which accounts for the bulk force $\rho_{el}E$ arising from the influence of the electric field E on the mobile ionic charge of the double layer, $\rho_{el.}$ Soft particles carry polyelectrolytes on their surfaces, which are assumed to be penetrable to ionic fluxes and hydrodynamic flow. Accordingly, Brinkman equation[51] is used, which is essentially the Stokes equation with an added term, γu:

$$\eta\frac{d^2u}{dx^2} - \gamma u + \rho_{el}E = 0 \tag{1}$$

where η is the fluid dynamic viscosity, u is the velocity distribution within the polyelectrolyte layer, and γ is the friction coefficient for flow in the soft polyelectrolyte layer.

The electric potential distribution in almost all theories is either calculated numerically or determined from an analytical solution of the linearized PB equation. A useful exception is Ohshima's analytical solution for the nonlinearized PB equation.[31,52,53] In addition, Ohshima obtained a useful general solution of Brinkman equation in an integral form, where the integrand depends on the potential distribution $\psi(x)$.

The electrokinetic theory for "soft" particles developed by Ohshima[31] considers a spherical colloidal particle with a core diameter, a, coated with an ion-penetrable layer of polyelectrolytes with a thickness d. The outer diameter of the particle is $b = a + 2d$. The theory is based on the following main assumptions: (i) the inertial term in the Navier−Stokes equation is negligible as the Reynolds number of the liquid flow inside and outside the polyelectrolyte layer is very small; (ii) particle velocity is proportional to the electrical field (i.e., weak electrical field); (iii) the slipping plane is located on the particle core; (iv) the polyelectrolyte layer is uniformly permeable to the mobile ions in solution while the particle core is impermeable; (v) the polyelectrolyte layer at the particle surface is uniformly charged over its thickness such that the polyelectrolyte fixed charge density, ρ_{fix}, is constant over r; and (vi) the dielectric permittivities of the liquid (ϵ_r) inside and outside the polyelectrolyte layer are identical.

A general equation for the EPM, μ, is derived and based on two parameters specific to the particle polyelectrolyte layer. The first parameter is the fixed charge density in the polyelectrolyte layer:

$$\rho_{fix} = NZe \tag{2}$$

where N and Z are the number concentration and the valence of the dissociated functional groups in the polyelectrolyte layer, respectively, and e is the elementary electric charge. The second parameter is the electrophoretic softness, $1/\lambda$, given in length units. The Electrophoretic softness is defined as

$$\frac{1}{\lambda} = \left(\frac{\eta}{\gamma}\right)^{1/2} \tag{3}$$

For cases where $\kappa a/2 \gg 1$, $a/2 \gg d$, $\lambda d \gg 1$, and $\kappa d \gg 1$, with κ being the Debye−Hückel parameter, and when the relaxation effect of the electrical field on the particle double layer is neglected, the "soft" particle EPM is given by[31]

$$\mu = \frac{\epsilon_r\epsilon_0}{\eta}\frac{\psi_0/\kappa_m + \psi_{DON}/\lambda}{1/\kappa_m + 1/\lambda} + \frac{\rho_{fix}}{\eta\lambda^2} \tag{4}$$

with the outer surface potential ψ_0 (i.e., at $r = b$), the Donnan potential in the polyelectrolyte layer ψ_{DON}, and the Debye−Hückel parameter of the polyelectrolyte layer, κ_m, given by

$$\psi_0 = \frac{kT}{ze}\left(\ln\left[\frac{\rho_{fix}}{2zen^\infty} + \left\{\left(\frac{\rho_{fix}}{2zen^\infty}\right)^2 + 1\right\}^{1/2}\right] + \frac{2zen^\infty}{\rho_{fix}}\left[1 - \left\{\left(\frac{\rho_{fix}}{2zen^\infty}\right)^2 + 1\right\}^{1/2}\right]\right) \tag{5}$$

(48) Black, A. P.; Smith, A. L. *J. Am. Water Works Assoc.* **1965**, *57*, 485−491.
(49) Donath, E.; Budde, A.; Knippel, E.; Baumler, H. *Langmuir* **1996**, *12*, 4832−4839.
(50) Donath, E.; Walther, D.; Shilov, V. N.; Knippel, E.; Budde, A.; Lowack, K.; Helm, C. A.; Mohwald, H. *Langmuir* **1997**, *13*, 5294−5305.
(51) Brinkman, H. C. *Appl. Sci. Res., A* **1947**, 81.
(52) Ohshima, H.; Kondo, T. *Colloid Polym. Sci.* **1986**, *264*, 1080−1084.
(53) Ohshima, H.; Kondo, T. *Biophys. Chem.* **1990**, *38*, 117−122.

$$\psi_{DON} = \frac{kT}{ze}\left(\ln\left[\frac{\rho_{fix}}{2zen^{\infty}} + \left\{\left(\frac{\rho_{fix}}{2zen^{\infty}}\right)^2 + 1\right\}^{1/2}\right]\right) \quad (6)$$

$$\kappa_m = \kappa\left[1 + \left(\frac{\rho_{fix}}{2zen^{\infty}}\right)^2\right]^{1/4} \quad (7)$$

Here, ϵ_0 is the permittivity in a vacuum, k is the Boltzmann constant, T is the absolute temperature, and z and n^{∞} are the valence and bulk number concentration of the symmetrical electrolyte in solution. It can be shown from eqs 5 to 7 that, at low number concentration of functional groups, N, the potentials ψ_0 and ψ_{DON} become proportional to N, viz.,

$$\psi_{DON} = 2\psi_0 = \frac{kT}{ze}\frac{ZN}{2zn^{\infty}} \quad (8)$$

and

$$\kappa_m \approx \kappa \quad (9)$$

so that eq 4 becomes

$$\mu = \frac{\rho_{fix}}{\eta\lambda^2}\left[1 + \left(\frac{\lambda}{\kappa}\right)^2\frac{1 + \lambda/2\kappa}{1 + \lambda/\kappa}\right] \quad (10)$$

2.4. Application of Ohshima's Theory to Experimental Data. A curve fitting procedure was applied to experimental values of EPM as a function of electrolyte concentration to determine the electrophoretic softness, $1/\lambda$, and fixed charge density, ρ_{fix}, of our bacterial cells. Both the general equation (eq 4) and the simplified equation for low potentials (eq 10) were used to model the experimental EPM data. The fitting procedure followed the Levenberg−Marquardt method (Matlab 5.0, The Mathworks).

2.5. Particle Deposition Kinetics. The deposition kinetics of the "hard" silica particles were determined by a radial stagnation point flow (RSPF) system. Deposition rates were determined as a function of ionic strength using a flat quartz surface as the substrate. The deposition kinetics data of the two bacterial strains were determined similarly and can be found in our recent publication.[45]

2.5.1. Collector Quartz Media. Round quartz cover slips of 25 mm diameter and 0.1 mm thickness (Electron Microscopy Sciences, Ft. Washington, PA) were cleaned by soaking in a 2% Extran MA02 solution (EM Science, Gibbstown, NJ), followed by a thorough rinsing with ethanol (Pharmco Products, Inc., Brookfield, CT) and deionized water. Next, the quartz slips were sonicated (10−15 min) while submerged in a 2% RBS 35 detergent solution (Pierce, Rockford, IL) followed by a second rinse with ethanol and DI water. The cover slips were soaked overnight in NOCHROMIX solution (Godax Laboratories, Inc., Tacoma Park, MD) and then rinsed thoroughly with deionized water. For deposition experiments under favorable electrostatic conditions, the slides were chemically modified with aminosilane. In this surface modification procedure, one side of the quartz cover slip was exposed to a 0.2% (vol/vol) mixture of (aminoethylaminomethyl)-phenethyltrimethoxysilane (Gelest, Inc., Tullytown, PA) in ethanol for 3−5 min at room temperature and then cured for 90 min at 130 °C. The slide was rinsed with deionized prior to use in the radial stagnation point flow cell.

2.5.2. Radial Stagnation Point Flow (RSPF) System. The system comprises a specially blown glass flow chamber installed on the stage of an optical microscope (Axioplan 2, Zeiss, Thornwood, NY). The silica particle suspension entered the radially symmetric flow cell through a 2-mm inner diameter capillary tube oriented in an upward direction. Flow impinged upon a microscope cover glass 2 mm above the capillary opening and traveled radially along the cover slide, exiting the RSPF chamber through a separate capillary tube. Deposition of the silica particles was recorded with a CCD camera (CCD-300-IFG, Dage MTI, Michigan City, IN) acquiring images every minute over the course of a 20 min injection, and analyzed with an image analysis software (KS400, Zeiss, Thornwood, NY). The number of deposited silica particles over a 106 μm × 80 μm area at the stagnation point region was determined for each image by comparing the changes between successive images.

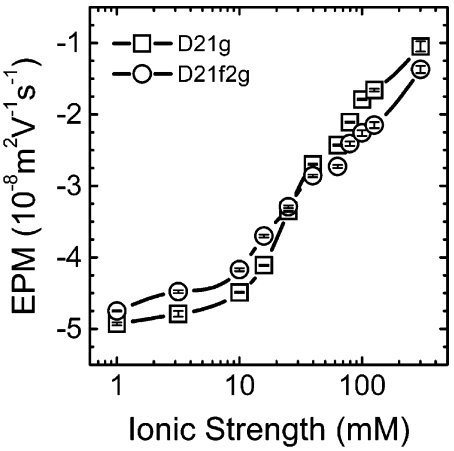

Figure 1. Electrophoretic mobility (EPM) as a function of ionic strength (KCl) for the two model *E. coli* strains. Experiments were carried out at an ambient pH (5.5−5.7) and a temperature of 22 °C.

Silica particle deposition experiments in the RSPF system were conducted over a range of ionic strengths (KCl) with a particle concentration of 10^7 particles/mL. All deposition experiments were conducted at least three times. Deposition experiments were performed at a flow rate of 5 mL/min corresponding to a capillary Reynolds number of 26.5 and a particle Peclet number of 0.931. For all experiments, the pH was unadjusted (ambient pH of 5.5−5.7) and the temperature was fixed at 22 °C (± 1 °C).

2.5.3. Determination of Particle Deposition Rate and Attachment Efficiency. Particle deposition onto the quartz surface in the radial stagnation point flow system is presented as a transfer rate coefficient, k_D. It is related to the particle deposition flux (number of particles per area per time), J, and the bulk particle concentration, C_0, via

$$J = k_D C_0 \quad (11)$$

The particle deposition flux was determined by normalizing the initial slope of the number of deposited particles versus time curve by the microscope viewing area. The deposition kinetics of the silica particles were also presented in terms of the attachment efficiency, α. The latter was calculated by normalizing the actual particle transfer rate coefficient at each ionic strength by the particle transfer rate coefficient obtained under favorable electrostatic conditions, $k_{D,fav}$:

$$\alpha = \frac{k_D}{k_{D,fav}} \quad (12)$$

3. Results and Discussion

3.1. Electrophoretic Mobility of the Model Bacterial Cells. The EPM as a function of ionic strength (KCl) for the two bacterial strains is shown in Figure 1. The two strains have a negative EPM reflecting their net negative surface charge originating from acidic functional groups on the LPS and transmembrane proteins. The EPM becomes less negative as the ionic strength increases because of charge screening by counterions and compression of the diffuse double layer.[54] At low salt concentration the dependence of the bacterial EPM on ionic strength is less pronounced, presumably due to the presence of co-ions and concentration polarization in the polyelectrolyte layer at the bacterial surface.[54,55] This behavior is in marked contrast with the classical double layer theory

(54) Elimelech, M.; O'Melia, C. R. *Colloids Surf.* **1990**, *44*, 165−178.
(55) Dukhin, S. S. *Adv. Colloid Interface Sci.* **1993**, *44*, 1−134.

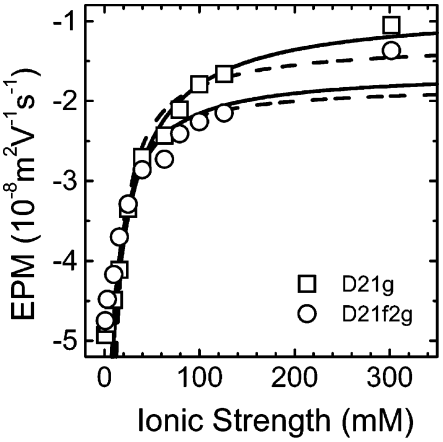

Figure 2. Electrophoretic mobilities (EPM) of the model bacterial strains fitted with the extended Ohshima's equation, eq 4 (solid line), and the simplified equation for low potentials, eq 10 (dashed line). Experimental conditions are described in Figure 1.

Table 1. Calculated Adjusted *R*-squared Values of the Fitting of the EPM Experimental Data by either Ohshima's Equation (eq 4) or the Simplified Equation for Low Surface Potentials (eq 10)

particle type	Ohshima's equation fit	simplified equation fit
D21g	0.984	0.939
D21f2g	0.879	0.828
silica	0.930	0.918

which predicts a continuous decrease in the electrokinetic potential with increasing salt concentration.[17]

A striking feature of the EPM at a very high ionic strength (300 mM) is the attainment of nonzero negative values. This residual EPM has been described as resulting from an electroosmotic electrolyte flow through the polyelectrolyte layer of soft particles.[56] The electrical body force induces a hydrodynamic drag force acting on the polymer segments and the interstitial fluid resulting in a slip velocity inside the polyelectrolyte layer.[57] This internal electroosmotic flow results in a residual finite EPM that depends only on the fixed charged density and permeability of the polyelectrolyte layer at the particle surface.

The EPMs of D21g and D21f2g are comparable over the studied ionic strength range. The results suggest that for these strains, the outermost boundary of the soft layer in contact with the bulk electrolyte solution has similar characteristics, such as charge density, despite the overall differences in morphology and surface charge density of the whole LPS layer. The trends for our two model strains are similar to published EPM data for the same strains.[45]

3.2. Application of the Electrophoretic Model for "Soft" Particles to EPM Data. The electrophoretic softness and fixed charge density of our model bacterial cells were determined by fitting Ohshima's electrophoretic theory for "soft" particles to the experimental EPM data. The fits of EPM for the two bacterial strains by Ohshima's equation (eq 4) and its simplified form (eq 10) are shown in Figure 2. The corresponding adjusted *R*-squared values are presented in Table 1. Best fits were obtained by considering only EPM data at ionic strengths above 15 mM, since inclusion of low ionic strength EPM data resulted in a poorer fitting. Sonohara and co-workers[36] have observed such deviation of Ohshima's theory from

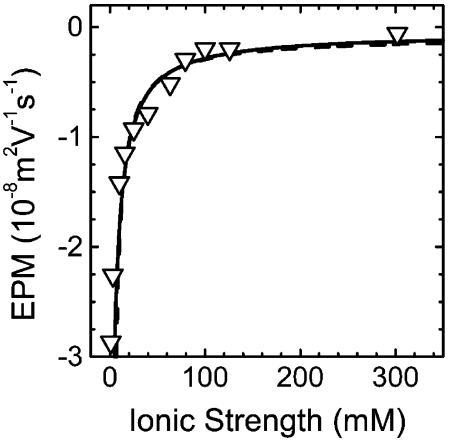

Figure 3. Electrophoretic mobilities (EPM) of the silica particles fitted with the extended Ohshima's equation, eq 4 (solid line), and the simplified equation for low potentials, eq 10 (dashed line). Experimental conditions are similar to those described in Figure 1.

Table 2. Calculated Values of Electrophoretic Softness and Fixed Charge Density for the Model Bacterial Strains and Silica Particles by Fitting Experimental EPM Data with Ohshima's Theory (eq 4)

particle type	fixed charge density ρ_{fix} (mM)	electrophoretic softness $1/\lambda$ (nm)
D21g	−149.9	0.74
D21f2g	−72.1	1.49
silica	−41.1	0.32

experimental EPM for the same bacterial species when considering ionic strengths below 50 mM, and explained it by the hydration of the LPS sugar monomers.

The full equation (eq 4) yields the best fitting of our experimental data. The differences between the full and simplified models regarding the applicability to the bacterial strains are reflected in the variation of the adjusted R-squared values of the EPM fittings (Table 1). The low potential approximation (eq 10) is thus not valid for the two bacterial strains.

To further test the validity of the model, a silica particle suspension was selected as a model for negatively charged hard particles. The silica particles exhibited relatively low EPM values and their residual EPM tends to zero at high ionic strength (Figure 3), as the Smoluchowski-Huckel equation predicts for "hard" spheres.[17] The low surface potential of the silica particles allows very good fitting of the experimental EPM by both the full and simplified models over the entire ionic strength range.

The parameters of the polyelectrolyte layer defined in the electrophoretic theory for soft particles have been determined for each particle type and are summarized in Table 2. A discussion on the relevance of these parameters to the actual surface features of the two bacterial strains is presented in the next section. The control silica particles show the expected trends in softness and fixed charged density for hard rigid spheres. The absence of a polyelectrolyte layer at the surface of the silica particles leads to an electrophoretic softness close to zero.

3.3. Relating Electrokinetic Parameters to Bacterial LPS Features. The electrophoretic softness and the fixed charge density have been used to characterize the structure of bacterial cell surface polyelectrolytes.[27,35,36,39,43,58,59] In a recent study it has been suggested that the calculated electrokinetic parameters do not correlate with the known surface characteristics of the studied bacterial strains.[40] The two bacterial strains selected for this study should allow a more systematic

(56) Ohshima, H. *Adv. Colloid Interface Sci.* **1995**, *62*, 189−235.
(57) Hill, R. J.; Saville, D. A.; Russel, W. B. *J. Colloid Interface Sci.* **2003**, *258*, 56−74.

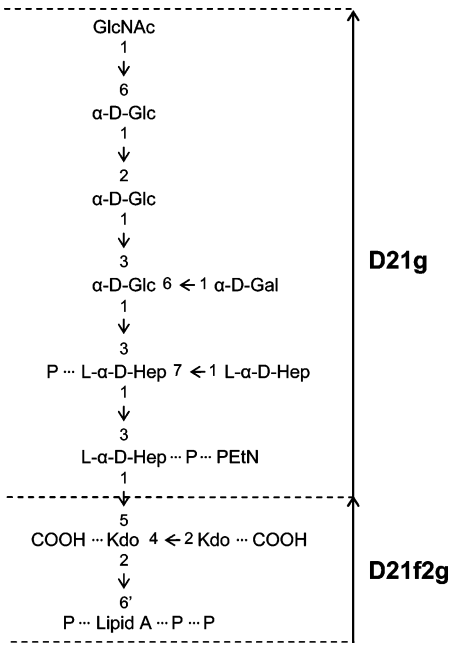

Figure 4. Carbohydrate backbone of the lipopolysaccharide (LPS) layer of the model bacterial strains: D21g and D21f2g. P indicates phosphate and PEtN indicates phosphoethanolamine. The dashed chemical bonds specify the presence of charged chemical groups (P, PEtN, and COOH). Adapted from Holst et al.,[63] Kanipes et al.,[62] Kato,[64] and Ong and al.[61]

and meaningful examination of the relevance of the electrophoretic softness and fixed charge density to describe surface features of bacterial cells.

The first model *E. coli* strain that we analyzed is the rough mutant D21g. It has a truncated LPS molecule with a length up to 4 nm,[60] comprising the lipid A, the KDO molecules, and the core polysaccharide (Figure 4).[61−64] These sections of the LPS are known to carry negatively charged groups, such as phosphates attached to the lipid A moiety, carboxylates of the KDO moieties, and phosphates attached at the heptose sugars.[44] The obtained fixed charge density and electrophoretic softness for this mutant are −149.9 mM and 0.74 nm, which are, respectively, the highest and smallest calculated values among the two bacterial strains (Table 2). The general trend of high fixed charge density and small, but different from zero, electrophoretic softness corresponds to the known characteristics of the truncated and highly charged LPS.

The second strain, D21f2g, is genetically related to D21g. D21f2g is a deep-rough mutant with a highly truncated form of the LPS molecule (Figure 4). The length of the LPS molecule was reported to be on the order of 1 nm,[44] which is less than the Debye screening lengths at the investigated ionic strengths. The LPS consists of lipid A anchoring the molecule to the outer membrane, and exposed hydrophilic KDO molecules.[62,63] The small size of the LPS molecule allows the exposure of other surface structures to the electrolyte solution, such as the outer membrane phospholipid bilayer that we assume to be impermeable to the electrolyte solution, and/or some hydrophilic sections of transmembrane proteins. Because the polyelectrolyte layer thickness is smaller than the Debye length, the EPM behavior of the D21f2g cells should, in principle, approach a behavior similar to that of hard particles. However, as shown in Table 2, the fitting of EPM data with Ohshima's equation gives non-negligible values of −72.1 mM for fixed charge density and 1.49 nm for electrophoretic softness. The values of these parameters should be comparable to the silica particles, for which we found a fixed charge density of −41.1 mM and an electrophoretic softness of 0.32 nm. It is likely that the fixed charge density is contributed by the charged outer membrane proteins, in addition to the charges found on the lipid A and KDO molecules. Ohshima's theory also predicts an electrophoretic softness higher than that for D21g, which means a higher permeability to fluid flow through the polyelectrolyte layer of D21f2g. The known morphological features of the D21f2g surface do not explain this high permeability; neither the phospholipid bilayer nor the transmembrane proteins should have such pronounced ionic permeability. It seems that the significance of both calculated parameters becomes questionable when the polyelectrolyte layer is thin and reaches the size of the Debye screening length.

3.4. Prospective Surface Potentials for Bacterial Cells. To predict bacterial electrostatic interactions with solid interfaces, it is critical to determine the electrical surface potential that actually governs such interactions. For soft particles, like bacterial cells, two different surface potentials are considered—the zeta potential and the outer surface potential.

3.4.1. Zeta Potential. The zeta potential is the electrical potential located at the hydrodynamic shear plane. For hard spherical particles, the zeta potential is assumed to be close enough to the particle core to represent the surface potential in predictions of electrostatic double layer interactions.[17] However, the presence of the ion-permeable polyelectrolyte layer at the surface of soft particles shifts the shear plane away from the particle core and greatly influences the distribution of the electrical potential across the soft polyelectrolyte layer.[56] Furthermore, migration of accumulated counterions in the permeable layer at high ionic strength induces an electroosmotic flow that imparts a residual EPM for the soft particle.[57] Consequently, the zeta potentials directly calculated from the measured EPM values do not approach zero at high ionic strength, as is the case for hard spherical particles. This phenomenon of substantial residual EPM (or zeta potential) at high ionic strength casts doubt on the suitability of the zeta potential as a representative surface potential for soft particles. The electric surface potential that represents the electrostatic double layer interactions of colloidal particles should tend to zero at high ionic strength, so it correctly predicts the absence of electrostatic double layer repulsive interactions with charged solid surfaces. However, despite the shortcomings, the zeta potential is still the most commonly used electrical potential to predict electrostatic double layer interactions between soft biological cells and solid interfaces.[65−68]

3.4.2. Outer Surface Potential. Ohshima's electrophoretic theory for soft particles allows the calculation of

(58) Skvarla, J.; Kupka, D.; Navesnakova, Y.; Skvarlova, A. *Folia Microbiol. (Prague)* **2002**, *47*, 218−224.
(59) van der Wal, A.; Norde, W.; Zehnder, A. J. B.; Lyklema, J. *Colloids Surf. B* **1997**, *9*, 81−100.
(60) Kastowsky, M.; Gutberlet, T.; Bradaczek, H. *J. Bacteriol.* **1992**, *174*, 4798−4806.
(61) Ong, Y. L.; Razatos, A.; Georgiou, G.; Sharma, M. M. *Langmuir* **1999**, *15*, 2719−2725.
(62) Kanipes, M. I.; Lin, S. H.; Cotter, R. J.; Raetz, C. R. H. *J. Biol. Chem.* **2001**, *276*, 1156−1163.
(63) Holst, O.; Zahringer, U.; Brade, H.; Zamojski, A. *Carbohydr. Res.* **1991**, *215*, 323−335.
(64) Kato, N. *Micron* **1993**, *24*, 91−114.
(65) Poortinga, A. T.; Bos, R.; Norde, W.; Busscher, H. J. *Surf. Sci. Rep.* **2002**, *47*, 3−32.
(66) Meinders, J. M.; vanderMei, H. C.; Busscher, H. J. *J. Colloid Interface Sci.* **1995**, *176*, 329−341.
(67) Hayashi, H.; Tsuneda, S.; Hirata, A.; Sasaki, H. *Colloids Surf., B* **2001**, *22*, 149−157.
(68) Bos, R.; Busscher, H. J. *Colloids Surf., B* **1999**, *14*, 169−177.

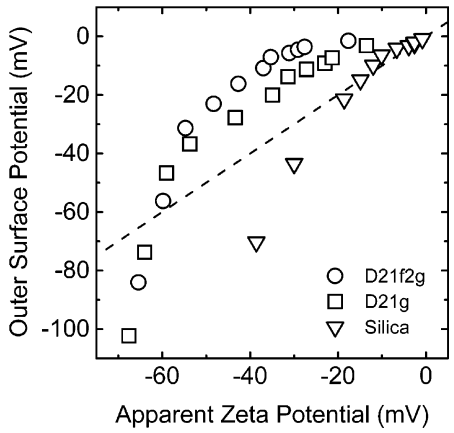

Figure 5. Outer surface potential versus apparent zeta potential for the model bacterial strains and the silica particles. The outer surface potentials were determined from the fitting of the measured electrophoretic mobilities to Ohshima's theory. The apparent zeta potentials were calculated directly from the measured electrophoretic mobilities using the Smoluchowski equation.

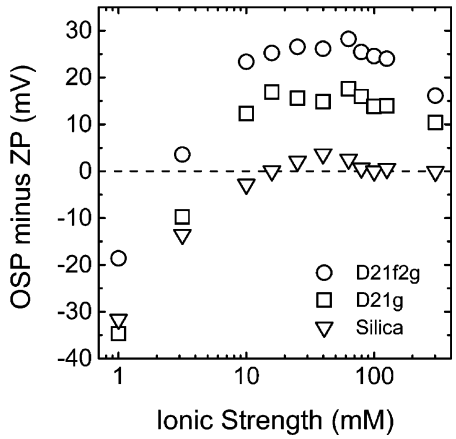

Figure 6. Difference between the outer surface potential (OSP) and the apparent zeta potential (ZP) as function of ionic strength for the model bacterial strains and silica particles. Data used from Figure 5.

the outer surface potential (eq 5)—the potential at the outermost boundary of the ion-permeable layer in direct contact with the surrounding electrolyte solution. It has been suggested that the outer surface potential is the proper electrical potential to use to predict electrostatic interactions between the soft particle surface and solid interfaces.[30] The outer surface potential has already been widely used to describe bacterial cell attachment to solid surfaces.[38,42,65,67,69] However, the physical meaning of the outer surface potential and its significance in predicting bacterial attachment has never been verified.

The outer surface potentials for the bacterial cells and silica particles were obtained from fitting the EPM data to Ohshima's theory (eqs 4−6). We also calculated the apparent zeta potentials utilizing the above EPM data with the classic Smoluchowski equation. These two sets of data are compared in Figure 5. For the three particle types, different behaviors of the outer surface potential can be observed. At very low ionic strength (1 to 3 mM), a noticeable deviation is observed between Ohshima's outer surface potential and the apparent zeta potential for each of the selected particles. The outer surface potential is more negative than the apparent zeta potential. It reflects the deviation from linearity in the variation of EPM at low ionic strength (Figure 1). Whereas the apparent zeta potential is directly proportional to the EPM of the particle, Ohshima's theory predicts a continuous decrease of the outer surface potential as the ionic strength increases. At high ionic strength, the outer surface potential tends to zero, as is the case for surface potentials of typical colloidal particles where screening and double layer compression suppress the surface potential. This behavior may imply that the outer surface potential is a likely candidate to predict electrostatic double layer interaction forces between soft particles and a solid surface, at least at high ionic strengths. For the silica particles, except at low ionic strengths (as discussed above), the outer surface potential is identical to the apparent zeta potential, so it may represent the real surface potential of the particle as the zeta potential does.

The outer surface potential for the model bacterial strains is obviously smaller (less negative) than the zeta potential. Because the outer surface potential represents the potential at the outermost boundary of the polyelectrolyte layer, the potential difference between the outer surface potential and the zeta potential corresponds to the potential increase or decrease between the shear plane and the boundary between the polyelectrolyte layer and the surrounding (bulk) solution. Thus, we may expect that this potential difference could be related to the length of the LPS, because the shear plane is located deeper in the soft layer, or even at the particle core surface as assumed by Ohshima's theory. However, as shown in Figure 6, the difference between the outer surface potential and the apparent surface potential is most significant for the D21f2g, the bacterial cell with the most truncated LPS. In fact, for D21f2g, the outer surface potential is, on average, 25 mV less negative than the apparent zeta potential at ionic strengths above 10 mM, whereas the potential difference for D21g over the same ionic range is on average only 15 mV. We can conclude that the surface potential difference is not related to the cell LPS morphology, suggesting that the shear plane for the model bacterial strains is not located at the particle core surface. The actual location of the plane of shear depends on the properties of the ion-permeable layer, namely, the permeability to the bulk solution and the fixed charge density, as well as the particle core surface charge density.

3.5. Can Bacterial Deposition Kinetics Be Predicted Using the Cell Outer Surface Potential? One of the aims of the electrokinetic theory for soft particles is to define an electric surface potential that would be more relevant than the zeta potential to describe electrostatic interactions of soft particles. To verify the ability of the outer surface potential to predict bacterial adhesion (deposition) kinetics, we determined the apparent zeta potentials as well as the outer surface potentials for the two bacterial strains and the silica particles in the previous section. Under the solution conditions analyzed, the apparent zeta potentials and the outer surface potentials are negative for all particle types. Hence, one would expect electrostatic repulsion between these particles and a negatively charged surface, such as quartz. However, for soft particles, the outer surface potential and the zeta potential are different at moderate and high ionic strengths and, thus, would predict different behaviors of cell/particle deposition kinetics. The zeta potentials, which are calculated from the measured EPM data using the Smoluchowski equation, level off at a residual electrical potential. In this case, if the zeta potential represents the actual particle surface potential, electrostatic repulsion may prevail when the soft particle approaches a negatively

(69) McClaine, J. W.; Ford, R. M. *Appl. Environ. Microbiol.* **2002**, *68*, 1280−1289.

Table 3. Summary of the Electrical Potentials (Apparent Zeta Potential, ZP, and Outer Surface Potential, OSP) for the Three Particle Types and the Quartz Slide (only ZP) as Used in the DLVO Calculations for the Two Indicated Ionic Strengths (IS)

	quartz	D21g		D21f2g		silica	
IS (mM)	ZP (mV)	ZP (mV)	OSP (mV)	ZP (mV)	OSP (mV)	ZP (mV)	OSP (mV)
31.6	−13.60	−39.65	−24.39	−40.19	−13.83	−11.16	−8.38
100	−11.60	−13.00	−9.14	−29.10	−4.53	−2.60	−2.61

charged surface, and the predicted particle deposition rate would be low at high ionic strength. On the other hand, the calculated outer surface potential tends toward zero at high ionic strength, predicting the absence of electrostatic double layer repulsion with a charged solid interface. This indicates that in the absence of other repulsive interactions, such as steric repulsion, the soft particle will deposit at a particle-transfer limited rate.

3.5.1. Predicted DLVO Interaction Energy Profiles. To verify the relevance of both the apparent zeta potential and outer surface potential in predicting the bacterial surface interaction potential, DLVO theory is used to calculate the total interaction energy as a bacterial cell approaches a quartz surface. The calculated interaction energy profiles are used to interpret our previously published data of bacterial deposition kinetics on pure quartz slide in a radial stagnation point flow system (RSPF).[45] The total interaction energy, namely, the sum of the attractive van der Waals and repulsive electrostatic interactions, was calculated considering a sphere-plate system. Repulsive electrostatic double layer interaction energies were calculated using the constant surface potential expression of Hogg et al.[70] The expression for retarded van der Waals interaction proposed by Gergory[71] was used to calculate the attractive interaction energy. In the calculation of the van der Waals interaction energies, a Hamaker constant of 6.5×10^{-21} J was used for the bacterial cell−water−quartz system[72,73] whereas for the silica−water−quartz system a value of 1.7×10^{-20} J was employed.[74]

The interaction energy profiles are calculated using both the apparent zeta potentials and the outer surface potentials at ionic strengths of 31.6 and 100 mM. A summary of the electrical potentials at these ionic strengths is shown in Table 3. The variation of the DLVO interaction energy profiles as function of the electrical potential used, and at different ionic strengths, is illustrated in Figure 7. As shown, at 100 mM, DLVO theory predicts the absence of an energy barrier for the three particle types, regardless of the electrical surface potential used in the calculations. The absence of an energy barrier suggests fast (favorable) deposition rate of bacterial cells in a primary energy well. For an ionic strength of 31.6 mM, only the silica particles showed absence of an energy barrier for deposition, independent of the surface potential used in the calculations. At this ionic strength, the two model bacterial strains reveal a significant energy barrier to deposition when the apparent zeta potential is considered. The heights of the energy barriers are 157 kT for D21g and 153 kT for D21f2g. On the other hand, the use of the outer surface potential does not predict high energy barriers to cell deposition for

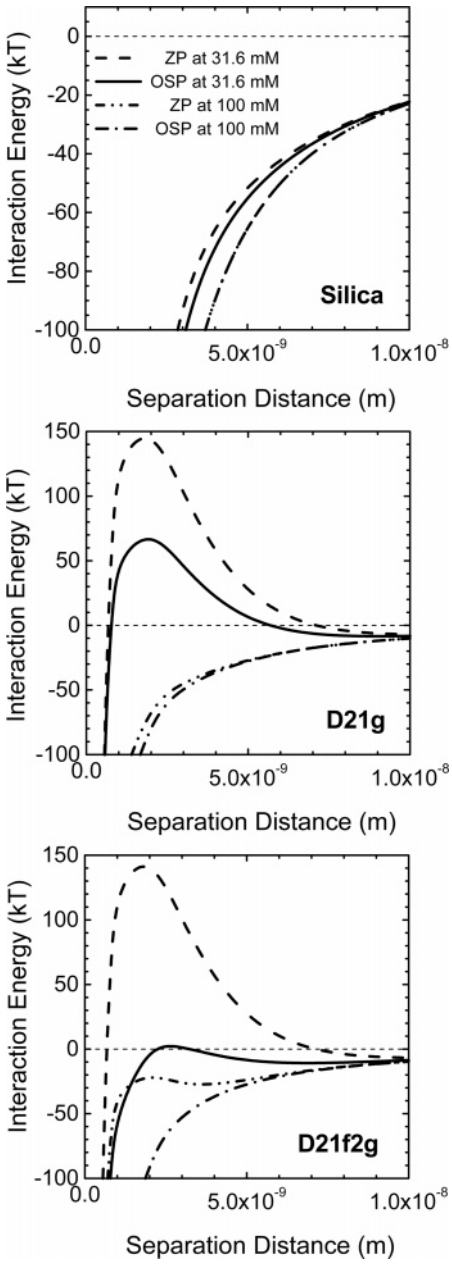

Figure 7. Calculated DLVO profiles as a function of ionic strength for the two model bacterial strains and the silica particles. Electrostatic interaction energies were calculated with either the outer surface potential or the apparent zeta potential (summarized in Table 3). The Hamaker constant was assumed to be 6.5×10^{-21} J for the bacteria−water−quartz interacting media, and 1.7×10^{-20} J for the silica−water−quartz interacting media. The equivalent particle diameters used in the calculations were 1.59 μm for the silica particle, 1.84 μm for D21g, and 1.77 μm for D21f2g. See text for more details.

any of the bacterial strains. In fact, at 31.6 mM, only D21g displays a substantial energy barrier (75 kT) that can prevent cell deposition in the primary minimum.

In the above calculations we assume that both the van der Waals and electrical double layer interactions start from the same zero separation distance, namely, from the core particle surface. However, for soft particles with polyelectrolyte layer on their surface—as our bacterial cells with their outer membrane LPS—proper consideration should be taken for the influence of the LPS layer on the electrostatic and van der Waals interactions. When van der Waals interactions are evaluated, the contribution of the LPS layer is negligible compared to the core of the

(70) Hogg, R.; Healy, T. W.; Fuerstenau, D. W. *Trans. Faraday Soc.* **1966**, *62*, 1638−1651.
(71) Elimelech, M.; O'Melia, C. R. *Langmuir* **1990**, *6*, 1153−1163.
(72) Truesdail, S. E.; Lukasik, J.; Farrah, S. R.; Shah, D. O.; Dickinson, R. B. *J. Colloid Interface Sci.* **1998**, *203*, 369−378.
(73) Simoni, S. F.; Bosma, T. N. P.; Harms, H.; Zehnder, A. J. B. *Environ. Sci. Technol.* **2000**, *34*, 1011−1017.
(74) Nguyen, A. V. *J. Colloid Interface Sci.* **2000**, *229*, 648−651.

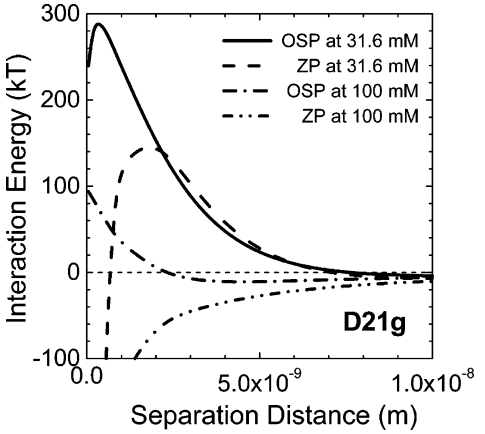

Figure 8. Calculated DLVO profiles for the model bacterial strain D21g considering the thickness of the LPS layer at the bacterial surface. Electrostatic interaction energies were calculated with either the outer surface potential or the apparent zeta potential (summarized in Table 3). The Hamaker constant and the equivalent diameter are similar to those described in Figure 7. The full length of the LPS molecule (4 nm) is the distance of closest approach between the quartz surface and the cell core. See text for more details.

bacterial cell; hence, the attractive van der Waals interactions should be calculated from the core particle surface. For electrostatic interactions, the apparent zeta potential should be considered at an interface located at the hydrodynamic plane of shear inside the LPS layer, whereas the outer surface potential is located at the outer boundary of the LPS layer in contact with the bulk electrolyte solution. This, however, poses serious difficulties since we do not know the *exact* thickness of the polyelectrolyte layer. As we discussed earlier in the paper, the D21f2g has a very short polyelectrolyte layer, most likely less than 1 nm, whereas the D21g cells have a polyelectrolyte layer of about 4 nm that is relatively uniformly charged.

To illustrate the effect of LPS thickness on the calculated DLVO interaction energy, we present such calculations for D21g in Figure 8. In these calculations, the outer surface potential starts at the external edge of the ion-permeable LPS layer, which was assumed to be fully extended (4 nm) at all ionic strengths. When using the zeta potential for calculations of electrostatic double layer interactions, the separation distance was assumed to start from the particle core surface, the assumed location of the hydrodynamic plane of shear based on Ohshima's theory. The van der Waals interactions, considered as taking place between the solid interface and the particle core, were calculated with the separation distance starting from the particle core. In this way, the full length of the LPS molecule is set as the distance of closest approach between the quartz surface and the cell core.

As shown in Figure 8, consideration of the LPS thickness in DLVO calculations results in interaction profiles predicting higher repulsive energies for our given experimental conditions. When the outer surface potential is considered as the surface potential, high energy barriers with no primary energy well are predicted at 31.6 and 100 mM ionic strength. The use of the apparent zeta potential as surface potential predicts an energy barrier at 31.6 mM, with a maximum of 157 kT, as well as a deep primary energy well at closer separation distance; no energy barrier is predicted at higher ionic strength (i.e., 100 mM). Such high repulsive interactions were not predicted in the previous analysis shown in Figure 7, where all interactions had the zero separation distance at the same plane, the bacterial core surface. It is, however, impossible to determine with accuracy the characteristic length of the LPS layer of our bacterial strains. Moreover, the LPS layer most likely changes conformation and length with changes in ionic strength, rendering such DLVO calculations intractable.

Table 4. Calculated Transfer Rate Coefficients (k_D) and Attachment Efficiencies (α) for the Model Bacterial Strains and Silica Particles at the Two Examined Ionic Strengths (IS)

particle type	IS (mM)	k_D (10^{-8} m/s)	α
D21g[a]	31.6	0.08 ± 0.03	0.00 ± 0.00
	100	0.56 ± 0.14	0.02 ± 0.01
D21f2g[a]	31.6	0.57 ± 0.36	0.06 ± 0.04
	100	3.30 ± 0.50	0.32 ± 0.05
silica	31.6	4.53 ± 0.33	0.90 ± 0.07
	100	4.38 ± 0.61	0.87 ± 0.12

[a] Data obtained by Walker et al.[45]

3.5.2. Relating Particle Deposition Kinetics to DLVO Interaction Predictions. Deposition kinetics of the two bacterial cells on a pure quartz slide in a radial stagnation point flow (RSPF) system have been studied by Walker et al.[45] The bacterial transfer rate coefficients, k_D, and the corresponding attachment efficiencies, α, for the two bacterial strains, along with deposition kinetics data obtained for the silica particles are summarized in Table 4. The RSPF system allows a direct visualization of deposition of the colloidal particles or bacterial cells onto a quartz cover slip. It has been shown that only cells that deposit irreversibly in a primary energy minimum are enumerated in the RSPF system.[75] Hence, the bacterial deposition rate in the RSPF system, and more specifically the attachment efficiencies (or the inverse of the stability ratios), should be related to the *actual* DLVO interaction energy profiles. This will allow us to critically assess the relevance of the zeta potential and the outer surface potential to predict electrostatic double layer interaction energies for bacterial cells.

Although the bacterial attachment efficiencies (Table 4) are relatively low for both ionic strengths examined, significant differences are seen between the two bacterial strains. Among the three particle types, the bacterial strain D21g exhibits the lowest attachment efficiencies, which stay close to zero for both ionic strengths. The two bacterial strains show significant increase in deposition rate (or attachment efficiency) upon increasing ionic strength from 31.6 to 100 mM. In contrast, the silica particles have an attachment efficiency close to unity at both ionic strengths.

The extremely low deposition rate for D21g indicates the presence of repulsive forces inhibiting bacterial attachment. Among the DLVO interaction energy profiles discussed in the previous section (Figure 7), both profiles at 31.6 mM ionic strength (i.e., profiles calculated with the zeta potential or the outer surface potential) show a significant energy barrier that can explain the observed deposition behavior. The apparent zeta potential results in an energy barrier about twice as much as that obtained with the outer surface potential, thus better explaining the absence of bacterial deposition at 31.6 mM under the conditions examined in the RSPF system. However, the absence of an energy barrier at 100 mM (Figure 7) does not corroborate with the very low attachment efficiency of D21g (Table 4). This behavior may suggest the presence of other repulsive forces, such as steric repulsion, attributed to the bacterial LPS macromolecules.

Accounting for the influence of the LPS thickness on the zero separation distance of the DLVO interactions, as

(75) Redman, J. A.; Walker, S. L.; Elimelech, M. *Environ. Sci. Technol.* **2004**, *38*, 1777−1785.

shown in Figure 8, demonstrates that, at both ionic strengths, only the outer surface potential predicts electrostatic energy barriers that are large enough to explain the low attachment efficiency for D21g. This may imply that the outer surface potential is the most representative electrical potential of the D21g cell surface. However, very little information is available on the LPS layer characteristics to allow the use of such DLVO predictions for our two model bacterial strains.

The bacterial strain, D21f2g, had a higher attachment efficiency than D21g. D21f2g has a low to moderate attachment efficiency at 31.6 mM ionic strength, and moderate to high attachment efficiency at 100 mM ionic strength. This deposition behavior suggests the presence of electrostatic repulsive forces between the cell surface and the solid interface, at least for the deposition run at 31.6 mM ionic strength. Contrary to the observations with D21g, only the apparent zeta potential for D21f2g predicts a substantial energy barrier at 31.6 mM that can explainthe slow deposition kinetics data for the cells (Table 3). At higher ionic strength (100 mM), both the zeta potential and the outer surface potential predict the absence of an energy barrier for D21f2g, which is somewhat in qualitative agreement with the attachment efficiency displayed in Table 3. The above results imply that the zeta potential remains a better approximation of the actual electric surface potential of our bacterial strains when the zero separation of the DLVO interactions is at the bacterial core surface.

Unlike the bacterial strains, the silica particles demonstrated good agreement between the predicted DLVO interaction profiles and the observed deposition rates (or attachment efficiencies) at both the low and high ionic strengths. The attachment efficiency of the silica particles was near unity at 31.6 and 100 mM ionic strengths, indicating the absence of repulsive energy barriers. In fact, our DLVO calculations clearly show that neither the use of the outer surface potential nor the zeta potential predict the presence of an electrostatic energy barrier that would inhibit deposition. Thus, for hard particles such as silica colloids, the outer surface potential becomes equivalent to the apparent zeta potential when the softness, $1/\lambda$, approaches zero as predicted by Ohshima theory (eq 4).[30]

3.6. Causes for the Failure of Electrokinetic Theory for "Soft" Particles. Application of Ohshima's theory to our experimental data demonstrated inconsistency with known features of the bacterial cells. The most likely causes for the failure of the electrophoretic theory for soft particles when applied to our bacterial cells are the chemical and physical heterogeneities associated with the ion-permeable polyelectrolyte layer at the cell surface. Such heterogeneities were omitted in the development of Ohshima's theory.

Chemical heterogeneity of the ion-permeable polyelectrolyte layer for our model bacteria refers to the nonuniform distribution of the charges in the radial direction across the LPS layer.[44,62] This chemical inhomogeneity directly contradicts one of the main assumptions of Ohshima's theory. The chemical heterogeneity also causes a nonuniform distribution of counterions and electric conductivity under the influence of electrical field, which has a direct impact on the cell surface potential.[76] Such chemical heterogeneity can be highly accentuated for a large number of Gram-negative bacteria, with a neutral or negatively charged O-antigen molecule ending the LPS.[77]

The surface conductivity of bacterial cells can be highly affected by specific activity of certain membrane proteins under extreme ionic strength conditions. Mechanosensitive channels in the inner membrane play an important role in ionic transfer during hypoosmotic shock to avoid cell lysis.[78,79] Several outer membrane proteins (Omp), such as OmpF, a large pore channel,[80] allow ionic exchanges between the periplasm and the bulk solution by electrodiffusion.[81,82] The release of co-ions by the cells due to the accumulation of counterions in the double layer in proximity of the core surface allows maintenance of a constant transmembrane potential and osmotic pressure. Hence, additional factors related to the cell membrane activity need to be taken into account when extreme ionic conditions are employed during EPM measurements of bacterial cells.

Significant lateral heterogeneity in the distribution of outer membrane LPS has been observed for *E. coli* cells. The LPS molecules share the bacterial surface with abundant OMPs, which take a significant fraction of the bacterial surface. It has been shown that the distribution of the OMPs follows various patterns that are dynamic as a function of the cell growth and division stage.[83] The distribution of LPS and OMPs creates lateral heterogeneity of surface charge, which has a marked impact on the bacterial adhesive properties.[84,85] In addition to charge heterogeneity, the alternation between LPS and OMP induces nonuniform permeability to the electrolyte solution at the bacterial surface. The OMP-covered surface allows the bulk ions to reach the outer membrane surface and thus has a high permeability, whereas the dense LPS patches have a much lower permeability to the electrolyte. In this case, the calculated softness from EPM measurements is meaningless because Ohshima's theory assumes a uniformly permeable polyelectrolyte layer.

4. Conclusion

To examine the applicability of Ohshima's electrophoretic theory for soft particles to model bacterial cells, two major aspects of the theory were critically analyzed: (1) the relevance of the calculated electrophoretic softness and fixed charge density to the known surface features of the model bacterial cells and (2) the ability of the theory to determine an electric surface potential that represents the electrostatic interaction of the cells with solid surfaces. By fitting measured EPM data to Ohshima's theory, the calculated softness and fixed charge density failed to reflect the known characteristics of the LPS layer for the model bacterial strains. Furthermore, the calculated outer surface potentials on the basis of Ohshima's theory were shown to be less negative than the apparent zeta potentials at ionic strengths above 10 mM. The corresponding DLVO interaction energy profiles calculated with the outer surface potentials predicted relatively low or absence of

(76) Dukhin, S. S.; Zimmermann, R.; Werner, C. *J. Colloid Interface Sci.* **2004**, *274*, 309−318.

(77) Ørskov, F.; Ørskov, I. In *Methods in Microbiology*; Bergan, T., Ed.; Academic Press: New York, 1984; Vol. 14, pp 43−112.

(78) Li, Y. Z.; Moe, P. C.; Chandrasekaran, S.; Booth, I. R.; Blount, P. *EMBO J.* **2002**, *21*, 5323−5330.

(79) Hamill, O. P.; Martinac, B. *Physiol. Rev.* **2001**, *81*, 685−740.

(80) Bransburg-Zabary, S.; Nachliel, E.; Gutman, M. *Solid State Ionics* **2004**, *168*, 235−243.

(81) Basle, A.; Iyer, R.; Delcour, A. H. *Biochim. Biophys. Acta* **2004**, *1664*, 100−107.

(82) Alcaraz, A.; Nestorovich, E. M.; Aguilella-Arzo, M.; Aguilella, V. M.; Bezrukov, S. M. *Biophys. J.* **2004**, *87*, 943−957.

(83) Gibbs, K. A.; Isaac, D. D.; Xu, J.; Hendrix, R. W.; Silhavy, T. J.; Theriot, J. A. *Mol. Microbiol.* **2004**, *53*, 1771−1783.

(84) Jones, J. F.; Feick, J. D.; Imoudu, D.; Chukwumah, N.; Vigeant, M.; Velegol, D. *Appl. Environ. Microbiol.* **2003**, *69*, 6515−6519.

(85) Walker, S. L.; Hill, J. E.; Redman, J. A.; Elimelech, M. *Appl. Environ. Microbiol.* **2005**, *71*, 3093−3099.

electrostatic repulsion, which could not explain the low deposition rate of the model bacterial strains on quartz surfaces. For the conditions of our experiments, the apparent zeta potentials were a better predictor for the bacterial deposition rate than the outer surface potentials. The failure of Ohshima's theory was attributed to chemical and physical heterogeneities of the soft LPS layer on the bacterial cells, namely, the nonuniform distribution of charged groups on the LPS macromolecule and the patch-like distribution of LPS at the bacterial surface. Such heterogeneities were not accounted for in the development of Ohshima's theory.

Acknowledgment. The authors acknowledge the support of the National Science Foundation, Collaborative Research Activities in Environmental Molecular Sciences (Grant CHE-0089156), and Professor H. P. Spaink (Leiden University, The Netherlands) for use of the EGFP plasmid.

LA047049T